

# Enhancement of magnetization plateaus in low dimensional spin systems

Alexandros Metavitsiadis,<sup>1,\*</sup> Christina Psaroudaki,<sup>2,3,†</sup> and Wolfram Brenig<sup>1,‡</sup>

<sup>1</sup>*Institute for Theoretical Physics, Technical University Braunschweig, D-38106 Braunschweig, Germany*

<sup>2</sup>*Department of Physics, California Institute of Technology, Pasadena, CA 91125, USA*

<sup>3</sup>*Institute for Theoretical Physics, University of Cologne, D-50937 Cologne, Germany*

(Dated: February 19, 2020)

We study the low-energy properties and, in particular, the magnetization process of a spin-1/2 Heisenberg  $J_1 - J_2$  sawtooth and frustrated chain (also known as zig-zag ladder) with a spatially anisotropic  $g$ -factor. We treat the problem both analytically and numerically while keeping the  $J_2/J_1$  ratio generic. Numerically, we use complete and Lanczos diagonalization as well as the infinite time-evolving block decimation (iTEBD) method. Analytically we employ (non-)Abelian bosonization. Additionally for the sawtooth chain, we provide an analytical description in terms of flat bands and localized magnons. By considering a specific pattern for the  $g$ -factor anisotropy for both models, we show that a small anisotropy significantly enhances a magnetization plateau at half saturation. For the magnetization of the frustrated chain, we show the destruction of the 1/3 of the full saturation plateau in favor of the creation of a plateau at half-saturation. For large anisotropies, the existence of an additional plateau at zero magnetization is possible. Here and at higher magnetic fields, the system is locked in the half-saturation plateau, never reaching full saturation.

## I. INTRODUCTION

Frustrating interactions in quantum magnets have revealed a plethora of exotic phenomena with no classical analogue [1, 2]. One such example is the appearance of magnetization plateaus, i.e., regions in the magnetization process of a paramagnetic system at which the magnetization stays put at some fractional value  $M_p$  of the saturation magnetization  $M_s$  despite the increase of the magnetic field. Magnetization plateaus have been observed in several systems independent of their dimensionality, described by very different geometries, e.g. in Shastry-Sutherland type of models [3–5], triangular [6–9], square [10, 11], checkerboard [12], Kagome geometries [13], down to one-dimensional (1D) frustrated systems [14, 15] and many more (see also Refs. [16–20] for comparative studies). While significant knowledge may have been gathered on the ground state of these systems, the situation often becomes more challenging at the magnetization plateau where a prerequisite for the existence of a plateau is the opening of a gap in some parts of the spectrum.

Here we use the sawtooth as well as the frustrated chain (see Fig. 1) as prototypical models to investigate the effect of a spatially modulated  $g$ -factor in systems that exhibit magnetization plateaus. Not only are these models the cornerstones of one-dimensional quantum magnetism but they have also been used to understand physics in higher dimensions. According to the Oshikawa-Yamanaka-Affleck theorem [21, 22], a one-dimensional spin- $S$  system with a  $p$ -periodic ground state, could exhibit magnetization plateaus for values of the magnetization  $M$  which satisfy the condition

$pS(1 - M/M_s) \in \mathbb{Z}$ . The sawtooth chain exhibits a magnetization plateau at half saturation  $M_p = M_s/2$  for a wide range of the ratio  $J_2/J_1$  [23], while the frustrated chain exhibits a magnetization plateau at  $M_s/3$  [24].

In this work, we primarily focus on the sawtooth chain, but we keep the analysis as general as possible to simultaneously treat the frustrated chain and discuss the similarities as well as the differences between the two models. Although the sawtooth chain, as well as variants of it, have been studied theoretically early on [25–39] they remain of great interest until today [40–45]. From an experimental point of view, the situation remains challenging, with only a limited number of compounds being reported until this day to materialize dominant magnetic interactions in a sawtooth pattern. Prominent examples are the delafossite  $\text{YCuO}_{2.5}$  [46–49], the double spin chain systems  $\text{KCuCl}_3$  and  $\text{TlCuCl}_3$  [15], the multiferroic  $\text{Mn}_2\text{GeO}_4$  [50–52], the olivines  $\text{ZnL}_2\text{S}_4$  ( $L = \text{Er, Tm, Yb}$ ) [53], and the Fe chains  $\text{Rb}_2\text{Fe}_2\text{O}(\text{AsO}_4)_2$  and  $\text{Fe}_2\text{O}(\text{SeO}_3)_2$  [54, 55]. Remarkably, and despite great efforts, a magnetization plateau has not been reported for any of these systems. Very recently, a study on the magnetic structure of the natural mineral atacamite showed that its magnetic structure is that of the sawtooth type with antiferromagnetic couplings between the spin-1/2 moments, with however a puzzling magnetization plateau [56].

Our paper is organized as follows. First, in Sec. II, we present the model and its basic properties. In the first part of our results, we present analytical calculations (Sec. III), first in terms of field theory, Secs. III A and III B, and then in terms of localized magnons in Sec. III C. In the second part of our analysis, we present numerical results (Sec. IV) for a uniform or modulated  $g$ -factor and for both the sawtooth as well as the frustrated chain. We conclude in Sec. V.

\* a.metavitsiadis@tu-bs.de

† cpsaroud@uni-koeln.de

‡ w.brenig@tu-bs.de

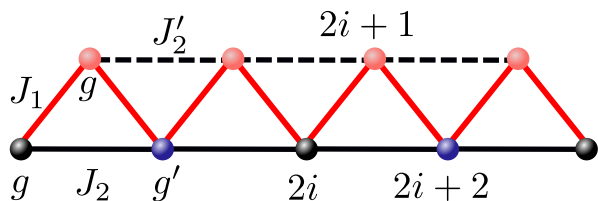


FIG. 1. A generalized 1D chain with anisotropic next nearest neighbor interactions. The upper base-base coupling is parametrized as  $J'_2 = (1 - \alpha)J_2$ , with  $\alpha = 0, 1$ . For  $\alpha = 0$  ( $J'_2 = J_2$ ) the frustrated chain with NNN interactions, or zig-zag ladder, is recovered while for  $\alpha = 1$  ( $J'_2 = 0$ ) the sawtooth chain is recovered. The  $g$ -factor is considered to be either uniform  $g' = g$  or to vary on every other site of the lower chain with  $g' = g - \delta g$  and  $\delta g > 0$ , indicated by black and blue colors. For the upper chain, we consider a uniform  $g$  value.

## II. MODEL

Our starting point is the generalized 1D Heisenberg chain with nearest  $J_1$  neighbor (NN) and anisotropic next nearest neighbor (NNN) interactions  $J_2$  and  $J'_2 = (1 - \alpha)J_2$ , Fig. 1. The Hamiltonian that describes this system in the presence of a uniform magnetic field along the  $z$ -axis  $\mathbf{B} = B\hat{z}$  reads

$$H = - \sum_j g_j \mu_B B S_j^z + J_1 \sum_j \mathbf{S}_j \cdot \mathbf{S}_{j+1} + \frac{J_2}{1 + \alpha} \sum_j [1 + (-1)^j \alpha] \mathbf{S}_j \cdot \mathbf{S}_{j+2}. \quad (1)$$

where  $\mathbf{S}_j$  are spin- $\frac{1}{2}$  operators residing on the lattice sites,  $\mu_B$  is the Bohr magneton, and we set  $\hbar = 1$ . We consider only two values for the parameter  $\alpha = 0$ , or 1. The sawtooth chain is recovered for  $\alpha = 1$  ( $J'_2 = 0$ ) and the frustrated chain (or zig-zag ladder) for  $\alpha = 0$  ( $J'_2 = J_2$ ) respectively. Although we are mainly interested in the case of the sawtooth chain, we keep  $\alpha$  as a parameter in our analysis to draw analogies between the two models. The ratio of the two couplings  $f = J_2/J_1$  can also be perceived as the degree of frustration. A central point of this work is our consideration of a particular spatial variation of the  $g$ -factor. Namely,  $g_j$  exhibits two patterns: a *uniform* one  $g_j = g$  and a *modulated* one, where the value of the  $g$ -factor on every second site of the lower chain has a different value  $g'$ , with  $g' = g - \delta g$  and  $\delta g > 0$ . In most material realizations, a possible finite  $\delta g$  is expected to be of the order  $\delta g/g \sim \mathcal{O}(0.1)$ . Despite that, here, we vary  $\delta g$  as a free parameter, letting  $g$  to acquire values as high as  $g$ , to provide a complete picture of our theoretical findings. Note that for  $\delta g > g$ , the  $g$ -factor exhibits a staggering sign. We would also like to stress that the sawtooth chain has no leg inversion symmetry, and therefore such a modulation only on one part of the system is not unlike to happen in material realizations.

The two models, the frustrated chain and the sawtooth chain share some common properties. They both exhibit either a unique gapless spin fluid (Tomonaga Luttinger

liquid) ground state, or a gapped dimerized one when the degree of frustration is in the range  $f_{c_1} < f < f_{c_2}$  [35, 57–59]. Both models allow for analytical solutions of their ground states at special values of the frustration ratio ( $f = 1$  for the sawtooth chain and  $f = 1/2$  for the frustrated chain) with double degenerate ground states [27, 60–62]. The low lying excitations are kink and anti-kinks in the form of domain walls spatially separating regions of one type of ground state. Their dispersion, however, differs with the kink excitations being gapped in the sawtooth and gapless in the frustrated chain [31]. Another difference between the two models appears in the magnetization process of each system. While the sawtooth chain exhibits a plateau at  $M_p = M_s/2$ , the frustrated chain exhibits one at  $M_p = M_s/3$ . For completeness, we mention that the value of the plateau  $M_p$  depends on the geometrical properties of the model and therefore is independent of the coupling ratio  $f$  in contrast to the plateau's width, which depends on the size of the gap in the presence of the magnetic field, and therefore depends on the degree of frustration.

## III. ANALYTICAL RESULTS

First, we treat the problem analytically by employing Abelian and non-Abelian bosonization focusing on the  $J_1 \gg J_2, J'_2$  regime.

### A. Non-Abelian bosonization

Let us first detour by revisiting the field theory of the sawtooth chain in the absence of a magnetic field in the context of non-Abelian bosonization [63–67]. Within non-Abelian bosonization, both the  $U(1)$  and the  $SU(2)$  symmetries of the underlying Hubbard model are considered in terms of the bosonic field  $\varphi_c$  and the matrix field  $\mathbf{g}$ . The charge sector is gapped out, and the spin operators can be written in terms of chiral  $SU(2)$  currents  $\mathbf{J}_{L/R}$  and the staggered magnetization  $\mathbf{n} = \text{Tr} \sigma \mathbf{g}$  as

$$\mathbf{S}(x) \approx \mathbf{J}_L(x) + \mathbf{J}_R(x) + (-1)^x \Omega \mathbf{n}(x), \quad (2)$$

where the bosonization constant  $\Omega$  is of the order of one, and it is related to the mass of the charge sector. The field theory is completed by considering one more additional operator, the dimerization  $\epsilon$ , given by the non-oscillating part of  $\epsilon(x) \sim (-1)^x \mathbf{S}(x) \cdot \mathbf{S}(x+a) \sim \text{Tr}(\mathbf{g})$  [65, 68].

In the  $J_1 \gg J_2, J'_2$  regime the system can be considered as a Heisenberg chain with a coupling constant  $J_1$  perturbed by the couplings  $J_2, J'_2$ , where each one of the latter couples NNN sites that belong only to one of the two sublattices (the upper or the lower chain). In the continuum, the perturbation of the fixed point Hamiltonian  $H_0(J_1)$  reads

$$\delta H = \frac{1}{1 + \alpha} \int dx [\lambda_J \mathbf{J}_L \cdot \mathbf{J}_R(x) + \lambda_{\partial\epsilon} \partial\epsilon(x)]. \quad (3)$$

The bare couplings  $\lambda$  depend on the microscopic couplings  $J_1, J_2, J_2'$  and the bosonization constant  $\Omega$

$$\lambda_J \sim J^c - J_2, \quad \lambda_{\partial\epsilon} \sim \alpha \frac{3\Omega^2}{2\pi} J_2,$$

with  $J^c$  the critical coupling for each model. The current operator is generated by the interaction term of the NN Hamiltonian as well,  $\sim \sum S_j^z S_{j+1}^z$ , and the NNN couplings modify its bare value. For the frustrated chain ( $\alpha = 0$ ), translation symmetry by one site is restored, and the Luttinger liquid fixed point is solely disturbed by the current operator, which is known to open a gap at  $J_{zz}^c/J_1 \approx 0.241167$  and drive the system in a dimerized phase [58]. On the other hand, for the sawtooth chain ( $\alpha = 1$ ), the strength of the current operator due to the NNN interactions is reduced by a factor of 1/2 while the  $\partial\epsilon$  operator appears. The effect of this operator, which is a total derivative, has triggered a big dispute in the literature [34, 69–72]. Leaving aside for a moment the  $\partial\epsilon$  operator, the operator contents of the two models are identical and the only difference arises in the bare coupling  $\lambda_J$ . This means that the sawtooth chain would undergo a phase transition to a gapped dimerized phase at  $J_{st}^c = 2J_{zz}^c \approx 0.48$ , which coincides remarkably with the value predicted from numerical simulations [35]. In retrospect, one can argue that the  $\partial\epsilon$  operator has no effect on the deformation of the critical lines and can, therefore, safely be ignored.

## B. Abelian bosonization

Next, we move to the case of interest, i.e., the sawtooth chain in the presence of a magnetic field with an anisotropic  $g$ -factor. Because of the presence of the magnetic field, SU(2) symmetry is broken, and we turn to Abelian bosonization [66, 67, 73]. The low energy properties of these systems in the presence of a uniform magnetic field have been described extensively in the literature [34, 39, 69, 70, 74, 75]. Here, we include only what is essential for our work.

In the standard Abelian Bosonization machinery, spin operators are described in terms of fermionic operators using a Jordan-Wigner transformation. The spectrum of the XY-NN-Hamiltonian is linearized around the Fermi points  $\pm k_F$  and slow varying chiral field operators are introduced in the continuum ( $x = ja$ )

$$\psi(x) \sim e^{ik_F x} \psi_R(x) + e^{-ik_F x} \psi_L(x). \quad (4)$$

The Fermi wavevector is given in terms of the magnetization  $M$  and the saturation magnetization  $M_s = L/2$ ,  $k_F = \frac{\pi}{2a}(1 - m)$ , with  $m = \frac{M}{M_s}$ ; for example  $k_F = \frac{\pi}{2a}$  for  $M = 0$  and  $k_F = \frac{\pi}{4a}$  for  $M = M_s/2$ . In turn, the  $\psi_{L,R}$  fields are expressed in terms of the U(1) bosonic fields  $\phi = \phi_R + \phi_L$  according to

$$\psi_R(x) = \frac{1}{\sqrt{2\pi a}} e^{-i\beta\phi_R(x)}, \quad \psi_L(x) = \frac{1}{\sqrt{2\pi a}} e^{+i\beta\phi_L(x)}, \quad (5)$$

with  $\beta$  a numerical constant, here  $\beta = \sqrt{4\pi}$ . The system is then described in terms of  $\phi$  and its dual field  $\theta = \phi_R - \phi_L$  with  $[\phi(x), \theta(x')] = -i\vartheta(x - x')$  and  $\vartheta$  the Heaviside step function.

Here we assume a spatially modulated  $g$ -factor, which exhibits an alternating pattern taking values  $g$  or  $g' = g - \delta g$  on the lower chain, as described in Fig. 1. The effect of this modulation is that some of the spins, the ones residing on the black sites of Fig. 1, experience an effective magnetic field which is reduced from the uniform value  $h = g\mu_B B$ , to a different value  $h' = g'\mu_B B$ . The site dependence of the effective magnetic field  $h(x)$  can be written as

$$h(x) = h - \frac{\delta h}{4} \left[ 1 + 2 \cos\left(\frac{\pi}{2a}x\right) + \cos\left(\frac{\pi}{a}x\right) \right], \quad (6)$$

with  $\delta h = \delta g\mu_B B$ . Therefore it becomes apparent that in Fourier space,  $h(x) = \sum_q h_q e^{iqx}$ , the effective magnetic field has a finite overlap not only at momentum  $q = 0$ , but at  $q = \pm \frac{\pi}{2a}$  and  $\pm \frac{\pi}{a}$  as well, with the corresponding Fourier components  $h_q = h - \frac{\delta h}{4}$ ,  $\frac{\delta h}{4}$ , and  $\frac{\delta h}{8}$ .

In the field theory representation, the system is described by the Tomonaga-Luttinger liquid (TLL) Hamiltonian  $H_0$ , perturbed by several operators

$$H = H_0 + \sum_j \int dx \lambda_j O_j(x), \quad \text{with}, \quad (7)$$

$$H_0 = \frac{v}{2} \int dx \left[ K [\partial\theta(x)]^2 + \frac{1}{K} [\partial\phi(x)]^2 \right],$$

and  $v = v(m, J_1, J_2)$ ,  $K = K(m, J_1, J_2)$  the Tomonaga-Luttinger (TL) parameters [69, 75]. The perturbative part of the Hamiltonian reads

$$O_1 = \partial\phi, \quad O_2^q = \cos[\beta\phi(x) - (2k_F - q)x], \quad (8a)$$

$$O_3 = \cos[2\beta\phi(x) - (4k_F - G)x - 2k_F a], \quad (8b)$$

$$O_4 = \cos[2\beta\phi(x) - (4k_F - G)x - 4k_F a], \quad (8c)$$

$$O_5 = \cos[2\beta\phi(x) - (4k_F - \pi/a)x - 4k_F a], \quad (8d)$$

with

$$\lambda_1 = -\frac{h_0}{\sqrt{\pi}} + C(\alpha, m, J_1, J_2), \quad \lambda_2^q = -\frac{h_q}{\pi a}, \quad (9a)$$

$$\lambda_3 = \frac{J_1}{2\pi^2 a}, \quad \lambda_4 \sim \frac{J_2}{2\pi^2 a(1 + \alpha)}, \quad \lambda_5 = \alpha \lambda_4. \quad (9b)$$

Several comments are in order regarding this rich operator content. (i)  $G$  is the reciprocal lattice vector which for a uniform chain reads  $G = \frac{2\pi}{a}$ . For a system with a unit cell involving  $\nu \geq 1$  sites, it is modified to  $G = \frac{2\pi}{\nu a}$ . (ii) The operators in Eq. (8a) arise due to the magnetic field whereas the rest from the Heisenberg interactions. (iii) The  $O_2^q$  operator depends on  $q$  due to the two Fourier components at  $q = \frac{\pi}{2a}$  and  $\frac{\pi}{a}$  of the effective magnetic field. Furthermore, there are two different  $\lambda_2^q$  for each  $q$  component. (iv) Not all of these operators survive at every magnetization and/or for any  $G$ . The rapidly oscillating factors in the arguments of the cosines make them

vanish under integration, unless the terms in the parentheses multiplying  $x$  vanish. (v) Four-fermion operators yield in the continuum operators that oscillate with a momentum  $q = 2k_F$  as well. Normally these terms oscillate and will vanish upon integration. However, for a non-vanishing  $\alpha$  their momentum dependence is modified to  $q = 2k_F - \pi/a$ , which vanishes for  $k_F = \frac{\pi}{2a}$  ( $m = 0$ ). One needs to be careful, since they could yield relevant operators [34, 76], however, at the plateau,  $k_F = \frac{\pi}{4a}$ , they oscillate and we drop them here for simplicity. (vi) At finite magnetization, namely away from half filling in the fermion representation, there are additional contributions to  $\lambda_1$  due to the finite chemical potential. These terms are incorporated in the constant  $C$ . (vii) Interactions modify the contribution of the next nearest neighbor umklapp terms, which arise also from their  $XY$  part of the spin Hamiltonian. Far from the non-interacting regime, the exact coefficients of the umklapp terms cannot be accurately established.

The operators in Eq. (8a) is more relevant than the cosine operators in Eqs. (8b)-(8d), which can be marginal, relevant, or irrelevant. This depends on the coefficient of  $\phi$  in their argument as well as on the TLL interaction parameter  $K$ . To determine the behavior of the cosine operators one needs to consider its behavior under the renormalization group where the momentum cut-off  $\Lambda$  is decreased according to  $\delta\Lambda(l) = -\Lambda(l)\delta l$ . Assuming the sine-Gordon Hamiltonian  $H = H_0 + g \int dx \cos[\gamma\phi(x)]$  the coupling  $g$  of the operator  $\cos \gamma\phi$  changes in first order according to  $\frac{\delta \ln g}{\delta \ln \Lambda} = d_\gamma - 2$ , with  $d_\gamma = \frac{K\gamma^2}{4\pi}$  the scaling dimension of this operator. This means that the cosine operator is relevant for  $d_\gamma < 2$ , marginal for  $d_\gamma = 2$ , and irrelevant for  $d_\gamma > 2$  [66, 76]. For example, for vanishing  $J_2 = 0$  where  $K = 1/2$ , the coefficient in the umklapp term in Eq. (8b) is  $\gamma = 2\beta = 2\sqrt{4\pi}$ , i.e.,  $d_{2\beta} = 2$ , namely the operator is marginal which agrees with the literature [73].

Let us now discuss the effect of the magnetic field combined with the site modulation of the  $g$ -factor. The magnetic field contribution is described in Eq. (8a). From there, we see that the strength of the  $\partial\phi$  operator is reduced from its uniform value  $h$  by  $\delta h/4$ . This operator tends to make the field fluctuate, preventing its pinning to some constant value, which in turn would open a gap, and the formation of a magnetization plateau would become possible. In other words,  $\partial\phi$  is responsible for destroying magnetization plateaus, and in the presence of the modulation is weakened. The second contribution of the magnetic field comes in the form of the cosine operator in the same equation where the spatial modulation of the  $g$ -factor yields the  $\cos\beta\phi$  term, which is always relevant since  $K < 2$  [74]. Therefore, since this operator is more relevant than the rest of the operators, it is highly probable to prevail under renormalization and drive the system in a gapped phase, when it is not oscillating. From the above, it becomes apparent that the  $g$ -factor modulation has a twofold effect on the interaction of the sawtooth with the magnetic field. First, it

reduces the strength of the operator destabilizing magnetization plateaus, and second, it yields new relevant operators that can stabilize magnetization plateaus.

#### *Sawtooth chain*

We now apply the above to the sawtooth chain ( $\alpha = 1$ ). For a uniform magnetic field ( $\delta h = 0$ ), the lattice periodicity is determined by the two-site unit cell of the microscopic model and, therefore  $G = \pi/a$ . The physics at zero magnetization has been described in terms of non-Abelian bosonization in Sec. III. As the uniform magnetic field increases, the  $\partial\phi$  operator, which can be absorbed by the substitution  $\phi \rightarrow \phi + \frac{\lambda_1 K}{v} x$ , drives the system to an incommensurate phase still described by a TLL fixed point. At some point, a gap opens due to the operators in Eqs. (8b)-(8d), and the system enters the plateau phase. This happens at  $m = 1/2$  where  $4k_F = G = \frac{\pi}{a}$  and the oscillating factors in the argument of the cosines vanish [69, 74].

By introducing the  $g$ -factor modulation, the reciprocal lattice vector becomes  $G = \frac{\pi}{2a}$  and the operators  $O_3$  and  $O_4$  do not contribute. Hence, there is a competition between the  $O_5$  and the more relevant  $O_2^{\pi/2}$  ( $d_\beta < d_{2\beta}$ ) which is expected under RG to reach first the strong coupling limit. The gap of the system scales as  $\Delta \sim e^{-\ell}$  where  $\ell$  is the point where the perturbative RG breaks down, and the system is no longer conformally invariant [73]. Therefore, since more relevant operators reach the strong coupling limit faster, one could expect a larger gap, meaning a broader magnetization plateau at  $m = 1/2$ . This can also be understood from the sine-Gordon model, where the soliton mass relates directly to the plateau width [75] and the soliton mass scales inversely proportionally to the argument of the cosine, at least to leading order in  $\gamma$ . As a side remark, we mention that the operator  $O_2^\pi$  survives at  $k_F = \frac{\pi}{2a}$ , albeit with a reduced bare coupling as compared to the coupling of  $O_2^{\pi/2}$ , and therefore with fine-tuning of the microscopic parameters a magnetization plateau at  $m = 0$  may, in principle, arise.

#### *Frustrated chain*

The frustrated chain ( $\alpha = 0$ ) at a uniform field is known to exhibit a magnetization plateau at  $m = 1/3$  due to an even less relevant umklapp operator [14, 24]. However, when the site modulation dependence of the  $g$ -factor is switched on, the periodicity of the model changes, now  $G = \frac{\pi}{2a}$ , and the more relevant operator  $O_2^{\pi/2}$  will be present and easily prevail. In fact, the rest of the operators in Eq. (8) vanish due to the oscillating factors in the argument of the cosine, and it can be safely assumed that the TLL fixed point is solely perturbed by the  $O_2^{\pi/2}$  operator. Therefore, a wide plateau is expected

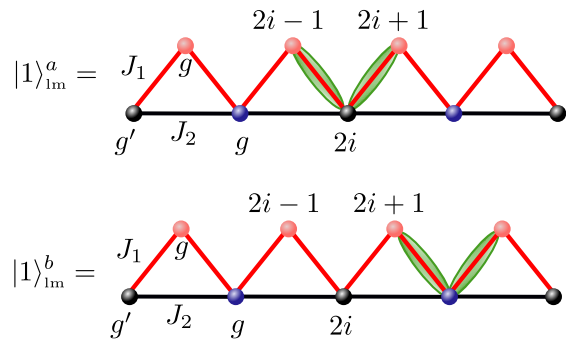


FIG. 2. Localized magnon states realized in the Heisenberg sawtooth chain. The magnon lives on the restricted area indicated by the green ellipses. State  $|1\rangle_{\text{lm}}^a$  with energy  $\varepsilon_1^a = h - 4J_2 - (2/3)\delta h$  is the lowest eigenstate in the sector  $M = L/2 - 1$ , while state  $|1\rangle_{\text{lm}}^b$  is a state with higher energy  $\varepsilon_1^b = h - 4J_2$ .

at  $m = 1/2$  instead of  $m = 1/3$ .

### C. Localized magnons

We now discuss how the magnetization plateau of the sawtooth chain can be explained in terms of localized magnons that emerge from the frustrated Hamiltonian of Eq. (1) due to a flat energy dispersion relation. Flat dispersions exist for several strongly frustrated spin lattices [19, 77], including the 2D Kagomé lattice [20] and 3D pyrochlore lattice [36], and frustrated electronic systems [78, 79].

We first note that in the subspace  $M = M_s = L/2$ , with  $L$  being the total number of spins, the fully polarized state  $|FM\rangle$  becomes the ground state for sufficiently large magnetic fields exceeding the saturation field  $h_{\text{sat}}$ , and plays the role of the vacuum state,  $|0\rangle = |FM\rangle$ , for the magnon excitations. For  $\delta g = 0$  the one magnon state reads

$$|1\rangle_k = \sum_{i=0}^1 \frac{1}{N_i} \sum_{j=1}^{L/2} e^{i2kj} S_{2j+i}^- |0\rangle, \quad (10)$$

where  $S^- = S^x - iS^y$ ,  $N_i$  normalization constants, and  $k = 4\pi \frac{l}{L}$ , with  $l \in \mathbb{Z}$  in the range  $[0, \frac{L}{2})$ . For  $f = 1/2$ , it corresponds to a completely flat magnon band  $\varepsilon_1 = h - 4J_2$  [23]. A complete flat dispersion suggests that one can construct a localized magnon state in a finite region of the lattice of the form

$$|1\rangle_{\text{lm}} = l_{2j}^\dagger |0\rangle = \frac{1}{\sqrt{6}} (S_{2j-1}^- - 2S_{2j}^- + S_{2j+1}^-) |0\rangle, \quad (11)$$

where the magnon is trapped in a valley indicated by the green ellipses in Fig. 2. Under general assumptions, one can demonstrate that  $|1\rangle_{\text{lm}}$  is the lowest eigenstate in the

sector  $M = M_s - 1$ , and becomes the ground state in an appropriate magnetic field [80, 81].

Due to the localized nature of state  $|1\rangle_{\text{lm}}$ , we proceed to fill the remaining of the lattice with  $n$  localized magnons  $|n\rangle_{\text{lm}} = l_{2j}^\dagger \dots l_{2j}^\dagger |0\rangle$ , states of lowest energy in the sector  $M = M_s - n$ , with energy  $\varepsilon_n = n\varepsilon_1 = n(h - 4J_2)$  above the energy of the ferromagnetic state. In order to avoid magnon-magnon interactions, magnons are constructed with sufficiently large space separation between them, and  $n$  cannot exceed  $n_{\text{max}} = L/4$ . We now allow for a finite but small  $\delta g > 0$ . Although states  $|n\rangle_{\text{lm}}$  are no longer eigenstates of the Hamiltonian, we can consider  $\delta g \ll g$ , and calculate their energy within first order perturbation theory. Two types of localized states can be realized, depending on whether the valley area is centered around a site with  $g'$  (black) or with  $g$  (blue) (see Fig. 2). After a straightforward calculation we find that states  $|n\rangle_{\text{lm}}^a$ , centered around a site with  $g'$ , have the lowest energy with  $\varepsilon_n^a = n(h - 4J_2 - (2/3)\delta h)$ , while states  $|n\rangle_{\text{lm}}^b$ , centered around a site with  $g$ , remain unaffected by  $\delta g$  and have energy equal to  $\varepsilon_n^b = n(h - 4J_1)$ . Thus, states  $|n\rangle_{\text{lm}}^a$  are the lowest energy states in the corresponding sector of magnetization  $M$ .

Under the assumptions specified above, at the saturation field,

$$h_{\text{sat}} = \frac{12g}{3g - 2\delta g} J_2, \quad (12)$$

there is a complete degeneracy of all localized-magnon states with energy  $\varepsilon_n = 0$ . As a result,  $m$  jumps between the saturation value  $m = 1$  and the value  $m = 1 - n_{\text{max}}/M_s = 1/2$ , with  $n_{\text{max}} = L/4$ . This is a macroscopic quantum effect, and the value of the jump vanishes if the spins become classical. The result above shows that a finite  $\delta g$  shifts the saturation field towards larger values, corroborating the field theory prediction for a larger plateau if  $\delta g \neq 0$ . For higher values of the anisotropy  $\delta g$ , first-order perturbation theory is expected to fail. The full treatment of the problem is involved and is done by means of second-order perturbation theory, taking into consideration the overlap of localized states and propagating states with energy higher than  $\varepsilon_n$ . However, this is beyond the scope of this work, and we leave it as a motivation for future studies.

## IV. NUMERICAL RESULTS

To test the previous theoretical findings, we resort to numerics. We employ two numerical methods, exact diagonalization (ED), namely full and Lanczos diagonalization, as well as the infinite Time Evolving Block Decimation (iTEBD) method [82, 83]. For ED we use symmetries, total  $S_z$  conservation, translation by two sites, spin flip for  $S_z = 0$ , and parity combined with translation by one site, to reduce the computational effort. In the presence of a uniform magnetic field, the energy levels of the system change according to  $E_n(h) = E_n(0) \pm hM$  where

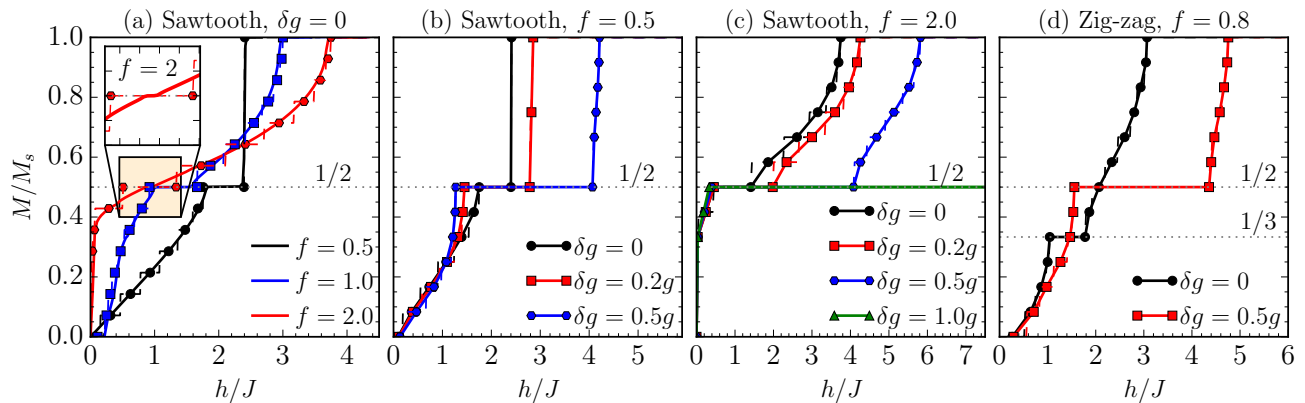


FIG. 3. (color online) Magnetization of the sawtooth (a-c) and the frustrated (d) chain versus the magnetic field. The magnetic field axis is rescaled by  $J = (2J_1 + J_2)/3$  for the sawtooth and by  $J = (J_1 + J_2)/2$  for the frustrated chain. (a) Comparison of the sawtooth magnetization obtained via ED for  $L = 28$  sites (thin dashed lines and points) to that obtained via iTEBD (thick solid lines) for three values of the frustration parameter  $f = 0.5, 1, 2$  and a uniform  $g$ -factor,  $\delta g = 0$ . The inset zooms in the highlighted region for  $f = 2$ . (b) Sawtooth magnetization via ED for  $L = 24$  and  $f = 0.5$  for three different values of the  $g$ -factor modulation,  $\delta g = 0, 0.2g, 0.5g$ . (c) Sawtooth chain's magnetization via ED for  $L = 24$  and  $f = 2$  for four different values of the  $g$ -factor modulation,  $\delta g = 0, 0.2g, 0.5g, g$ . (d) Frustrated chain's magnetization via ED for  $L = 24$  and  $f = 0.8$  for two different values of the  $g$ -factor modulation,  $\delta g = 0, 0.5g$ . The points in each panel and for each curve mark the middle of each magnetization step, except when a plateau is expected, where these points mark the beginning and the end of this step.

$E_n(0)$  is an eigenvalue of the Hamiltonian in the absence of the magnetic field. High energy states belonging to higher  $S_z$  sectors will lower their energy in the presence of the magnetic field and will become the ground state as the magnetic field reaches a certain value. This process for a finite system yields finite steps in the magnetization curve, which are not true plateaus but merely finite-size effects. In turn, one needs to discriminate between real magnetization plateaus and finite-size effects.

For a modulated  $g$ -factor, the situation becomes numerically more demanding. First, the unit cell is enlarged, which creates problems for both methods. Regarding ED, the number of  $k$ -points is reduced, meaning larger Hilbert spaces for each subsector, creating a memory threshold at smaller system sizes. An additional issue is that the energy levels in the presence of the magnetic field can no longer be evaluated parametrically from the levels without the magnetic field due to the site dependence of  $g_j$ . This means that each value of the magnetic field needs to be evaluated separately, leading to a dramatic increase of the computational time for the larger system sizes. Regarding iTEBD, the  $g$ -factor modulation causes convergence problems due to the larger unit cell. To avoid this, we rely solely on ED for  $\delta g > 0$ .

#### Sawtooth chain, uniform $g$ -factor

To correctly interpret the ED results, we first contrast the magnetization under a uniform magnetic field of a sawtooth chain for  $f = 0.5, 1, 2$  obtained via ED for  $L = 28$  spins to that obtained via iTEBD for an infinite system, Fig. 3(a). For all numerical simulations, we

assume  $h = B$ . For the ED results, we plot  $M(h)$  as dashed lines, exhibiting finite steps. It has been argued that connecting the middle point of these magnetization steps reproduces the magnetization curve in the thermodynamic limit. In Fig. 3(a), we also show the middle points of the magnetization steps, except at  $M_s/2$  where the plateau is expected, and we mark its limiting values. From the agreement of the points to the iTEBD data, one can safely argue that ED gives an excellent qualitative estimate of  $M(L \rightarrow \infty)$ . The only exception to that is the size of the plateau for  $f = 2$ , which ED tends to overestimate while from the iTEBD it seems rather small. To make this visible, we plot as an inset in panel Fig. 3(a) the magnetization for  $f = 2$  only in the highlighted region of the main panel. The disagreement between the two methods is attributed to the finite size behavior of the gap at elevated magnetic fields, which is rather small at this region of the parameter space.

Let us now describe the distinct features of the magnetization curve of the sawtooth chain for each value of frustration  $f$ . First, for the weakest  $J_1 = 0.5J_2$  ( $f = 2$ ), we observe a very steep increase of  $M$  at low magnetic fields. This reflects the two decoupled-chain limit  $J_1 \rightarrow 0$  where the upper spins, being loosely coupled with the rest of the system, can be very easily polarized. One additional point characteristic of the energy scales is that  $M(h)$  is a concave function of the magnetic field before the plateau and a convex function after it. A similar behavior is observed for  $f = 1$ , with a much wider plateau also apparent from the ED data [23]. As the ratio  $J_1 = 2J_2$  is further increased ( $f = 0.5$ ) the plateau still extends to a wide range of magnetic field range but the magnetization now displays a convex behavior for  $M(h) < M_s/2$ ,

and a concave one for  $M(h) > M_s/2$ . Hence, the sign of the second derivative of the magnetization  $\text{sgn}[M''(h)]$  provides a very useful criterion for the relative strength of the exchange couplings in the system. Decreasing further the ratio of the  $J_1/J_2$  would lead to a decrease in the size of the plateau, since the system comes closer to the non-frustrated Heisenberg chain [84].

In terms of localized magnons for  $f = 0.5$  (Sec. III C), and using Eq. (12), we find the saturation field to be  $h_{\text{sat}}/J = 4J_2/J = 2.4$ , for  $J = (2J_1 + J_2)/3$ , which is exactly the numerical value obtained from both methods. We also note that at the saturation field, there is a complete degeneracy of all localized-magnon states with energy  $\varepsilon_n = 0$ . As a result,  $m = M/M_s$  jumps between the saturation value  $m = 1$  and the value  $m = 1 - n_{\text{max}}/M_s = 1/2$ , with  $n_{\text{max}} = N/4$ .

### Sawtooth chain, modulated $g$ -factor

Now that the ED has been tested and its results can be correctly interpreted, we will use it to study the magnetization process in the presence of a spatially varying  $g$ -factor. In Figs. 3(b) and (c), we present results for the magnetization in the presence of a modulated factor for different deviations  $\delta g$  and for two values of the frustration ratio  $f = 0.5, 2$ , respectively. We observe that in both cases, a relatively small deviation of  $\delta g/g = 0.2$  already significantly extends the plateau region. As  $\delta g$  is further increased, the plateau grows even more while in the extreme case where  $\delta g \geq g$ , i.e., a  $g$ -factor with a staggering sign, the system is locked in the half-saturation plateau and never reaches full saturation. Classically thinking, this behavior is to be expected because the spins on the sites which have a  $g$ -factor of strength  $g$  will polarize faster. However, to satisfy the antiferromagnetic interactions of the system, the spins which experience a weaker magnetic field will order anti-parallel to the magnetic field to reduce the energy, and therefore the  $M_s/2$  plateau is favored. Lastly, we also observe that the  $g$ -factor modulation introduced here does not affect the sign of  $M''(h)$ , which seems to depend solely on the exchange couplings.

From Sec. III C and Eq. (12), the prediction for the values depicted in Fig. 3(b) is that  $h_{\text{sat}}/J = 2.8$  for  $\delta g = 0.2$ , which is in remarkably good agreement with the numerical results. For  $\delta g = 0.5$ , the theoretical prediction is  $h_{\text{sat}}/J = 3.6$ , which deviates from the numerical value  $h_{\text{sat}}/J = 4.1$ , suggesting that first-order perturbation theory employed here is insufficient. From Fig. 3(b) it also becomes apparent that for high values of  $\delta g$ , the degeneracy in  $n$  is lifted, and there is a number of critical fields  $h_{\text{cr}}(n)$  for which the magnetization  $M = M_s - n$  changes subsector, with  $1 \leq n \leq n_{\text{max}}$ . For the value of  $f$  chosen in Fig. 3(c) the picture of localized magnons holds

no longer and, therefore, no comparison to the theoretical predictions of Sec. III C can be made.

### Zig-zag ladder

Lastly, in the fourth panel of the magnetization data, Fig. 3(d), we apply the same idea but to the zig-zag ladder ( $J_2 = J'_2$ ), which is known to exhibit a plateau at  $M_s/3$  for a uniform magnetic field [14, 18]. Although the zig-zag ladder is invariant under chain inversion, the  $g$ -factor modulation considered here breaks chain reflection symmetry, enlarging the unit cell of the otherwise translationally-by-one-site invariant model to four. As one can see in Fig. 3(d), the plateau at  $M_s/3$  is destroyed in favor of creating a large plateau at  $M_s/2$ , as predicted by the field theory calculation.

## V. CONCLUSION

In conclusion, we presented a comprehensive theoretical study of the  $J_1 - J_2$  sawtooth as well as the frustrated chain focusing on their magnetization process. A unified field theory for both models was developed, and we demonstrated that by introducing a site dependence to the  $g$ -factor, the magnetization plateau of the sawtooth chain at  $M_s/2$  grows for any  $J_2/J_1$  ratio while the  $M_s/3$  plateau of the frustrated chain is destroyed in favor of a  $M_s/2$  plateau. For anisotropies where the  $g$ -factor vanishes or becomes staggered, we found that the system is locked in the  $M_s/2$  plateau, never reaching full saturation. We also emphasized the role of the curvature of  $M$  for acquiring an estimate of the microscopic couplings. We anticipate our results to provide guidelines for future theoretical and experimental studies, aiming in new ways to manipulate and extend the plateau region in frustrated magnets, including regimes where the plateau is expected to be small or even non-existing.

## VI. ACKNOWLEDGMENTS

We are thankful to Leonie Heinze for useful discussions, Xenophon Zotos for his comments on the sine-Gordon model, and Stefan Söllow for motivating this work. Work of W.B. has been supported in part by the DFG through Project A02 of SFB 1143 (Project-Id 247310070), by Nds. QUANOMET, and by the National Science Foundation under Grant No. NSF PHY-1748958. C.P. has received funding from the European Union's Horizon 2020 research and innovation programme under the Marie Skłodowska-Curie grant agreement No 839004. W.B. also acknowledges the kind hospitality of the PSM, Dresden.

- [1] L. Balents, *Nature* **464**, 199 (2010).
- [2] O. A. Starykh, *Reports on Progress in Physics* **78**, 052502 (2015).
- [3] B. S. Shastry and B. Sutherland, *Physica B+C* **108**, 1069 (1981).
- [4] Y. H. Matsuda, N. Abe, S. Takeyama, H. Kageyama, P. Corboz, A. Honecker, S. R. Manmana, G. R. Foltin, K. P. Schmidt, and F. Mila, *Phys. Rev. Lett.* **111**, 137204 (2013).
- [5] G. R. Foltin, S. R. Manmana, and K. P. Schmidt, *Phys. Rev. B* **90**, 104404 (2014).
- [6] A. V. Chubukov and D. I. Golosov, *Journal of Physics: Condensed Matter* **3**, 69 (1991).
- [7] A. I. Smirnov, H. Yashiro, S. Kimura, M. Hagiwara, Y. Narumi, K. Kindo, A. Kikkawa, K. Katsumata, A. Y. Shapiro, and L. N. Demianets, *Phys. Rev. B* **75**, 134412 (2007).
- [8] Y. Kamiya, L. Ge, T. Hong, Y. Qiu, D. L. Quintero-Castro, Z. Lu, H. B. Cao, E. S. Matsuda, M. Choi, C. D. Batista, M. Mourigal, H. D. Zhou, and J. Ma, *Nature Communications* **9**, 2666 (2018).
- [9] T. Ono, H. Tanaka, O. Kolomyiets, H. Mitamura, T. Goto, K. Nakajima, A. Oosawa, Y. Koike, K. Kakurai, J. Klenke, P. Smeibidle, and M. Meißner, *Journal of Physics: Condensed Matter* **16**, S773 (2004).
- [10] K. Morita and N. Shibata, *Journal of the Physical Society of Japan* **85**, 094708 (2016), <https://doi.org/10.7566/JPSJ.85.094708>.
- [11] M. E. Zhitomirsky, A. Honecker, and O. A. Petrenko, *Phys. Rev. Lett.* **85**, 3269 (2000).
- [12] K. Morita and N. Shibata, *Phys. Rev. B* **94**, 140404 (2016).
- [13] H. Nakano, Y. Hasegawa, and T. Sakai, *Journal of the Physical Society of Japan* **84**, 114703 (2015), <https://doi.org/10.7566/JPSJ.84.114703>.
- [14] K. Hida and I. Affleck, *Journal of the Physical Society of Japan* **74**, 1849 (2005), <https://doi.org/10.1143/JPSJ.74.1849>.
- [15] W. Shiramura, K.-i. Takatsu, H. Tanaka, K. Kamishima, M. Takahashi, H. Mitamura, and T. Goto, *Journal of the Physical Society of Japan* **66**, 1900 (1997), <https://doi.org/10.1143/JPSJ.66.1900>.
- [16] M. Takigawa and F. Mila, "Magnetization plateaus," in *Introduction to Frustrated Magnetism: Materials, Experiments, Theory*, edited by C. Lacroix, P. Mendels, and F. Mila (Springer Berlin Heidelberg, Berlin, Heidelberg, 2011) pp. 241–267.
- [17] A. Honecker, *Journal of Physics: Condensed Matter* **11**, 4697 (1999).
- [18] A. Honecker, J. Schulenburg, and J. Richter, *Journal of Physics: Condensed Matter* **16**, S749 (2004).
- [19] J. Richter, *Low Temperature Physics* **31**, 695 (2005), <https://doi.org/10.1063/1.2008130>.
- [20] J. Schulenburg, A. Honecker, J. Schnack, J. Richter, and H.-J. Schmidt, *Phys. Rev. Lett.* **88**, 167207 (2002).
- [21] M. Oshikawa, M. Yamanaka, and I. Affleck, *Phys. Rev. Lett.* **78**, 1984 (1997).
- [22] D. C. Cabra, A. Honecker, and P. Pujol, *Phys. Rev. Lett.* **79**, 5126 (1997).
- [23] J. Richter, O. Derzhko, and A. Honecker, *International Journal of Modern Physics B* **22**, 4418 (2008), <https://doi.org/10.1142/S0217979208050176>.
- [24] P. Lecheminant and E. Orignac, *Phys. Rev. B* **69**, 174409 (2004).
- [25] T. Hamada, J.-i. Kane, S.-i. Nakagawa, and Y. Natsume, *Journal of the Physical Society of Japan* **57**, 1891 (1988), <https://doi.org/10.1143/JPSJ.57.1891>.
- [26] K. Kubo, *Phys. Rev. B* **48**, 10552 (1993).
- [27] F. Monti and A. St, *Physics Letters A* **156**, 197 (1991).
- [28] T. Nakamura and Y. Saika, *Journal of the Physical Society of Japan* **64**, 695 (1995), <https://doi.org/10.1143/JPSJ.64.695>.
- [29] H. Otsuka, *Phys. Rev. B* **51**, 305 (1995).
- [30] T. Nakamura and K. Kubo, *Phys. Rev. B* **53**, 6393 (1996).
- [31] D. Sen, B. S. Shastry, R. E. Walstedt, and R. Cava, *Phys. Rev. B* **53**, 6401 (1996).
- [32] T. Nakamura and S. Takada, *Physics Letters A* **225**, 315 (1997).
- [33] K. Maisinger and U. Schollwöck, *Phys. Rev. Lett.* **81**, 445 (1998).
- [34] S. Chen, H. Büttner, and J. Voit, *Phys. Rev. Lett.* **87**, 087205 (2001).
- [35] Blundell, S. A. and Núñez-Regueiro, M. D., *Eur. Phys. J. B* **31**, 453 (2003).
- [36] J. Richter, J. Schulenburg, A. Honecker, J. Schnack, and H.-J. Schmidt, *Journal of Physics: Condensed Matter* **16**, S779 (2004).
- [37] M. Nakane, Y. Fukumoto, and A. Oguchi, *Journal of the Physical Society of Japan* **75**, 114712 (2006), <https://doi.org/10.1143/JPSJ.75.114712>.
- [38] K. Hida, *Journal of the Physical Society of Japan* **77**, 044707 (2008), <https://doi.org/10.1143/JPSJ.77.044707>.
- [39] S. Sarkar and C. D. Hu, *Phys. Rev. B* **77**, 064413 (2008).
- [40] Bellucci, S. and Ohanyan, V., *Eur. Phys. J. B* **75**, 531 (2010).
- [41] Z. Hao, Y. Wan, I. Rousochatzakis, J. Wildeboer, A. Seidel, F. Mila, and O. Tchernyshyov, *Phys. Rev. B* **84**, 094452 (2011).
- [42] X. Cai, S. Chen, and Y. Wang, *Phys. Rev. A* **87**, 013607 (2013).
- [43] J.-J. Jiang, Y.-J. Liu, F. Tang, C.-H. Yang, and Y.-B. Sheng, *Physica B: Condensed Matter* **463**, 30 (2015).
- [44] D. V. Dmitriev and V. Y. Krivnov, *Journal of Physics: Condensed Matter* **30**, 385803 (2018).
- [45] S. Paul and A. K. Ghosh, *Eur. Phys. J. B* **92**, 40 (2019).
- [46] R. Cava, H. Zandbergen, A. Ramirez, H. Takagi, C. Chen, J. Krajewski, W. Peck, J. Waszczak, G. Meigs, R. Roth, and L. Schneemeyer, *Journal of Solid State Chemistry* **104**, 437 (1993).
- [47] S. Capponi, C. Lacroix, O. L. Bacq, A. Pasturel, and M. D. Núñez-Regueiro, *Journal of Physics: Condensed Matter* **19**, 145233 (2007).
- [48] G. V. Tendeloo, O. Garlea, C. Darie, C. Bougerol-Chaillout, and P. Bordet, *Journal of Solid State Chemistry* **156**, 428 (2001).
- [49] O. Le Bacq, A. Pasturel, C. Lacroix, and M. D. Núñez-Regueiro, *Phys. Rev. B* **71**, 014432 (2005).
- [50] J. S. White, A. B. Harris, L. C. Chapon, A. Fennell, B. Roessli, O. Zaharko, Y. Murakami, M. Kenzelmann, and T. Kimura, *Nature Communications* **8**, 15457 (2017).



- [51] T. Honda, Y. Ishiguro, H. Nakamura, Y. Wakabayashi, and T. Kimura, *Journal of the Physical Society of Japan* **81**, 103703 (2012), <https://doi.org/10.1143/JPSJ.81.103703>.
- [52] J. S. White, T. Honda, K. Kimura, T. Kimura, C. Niedermayer, O. Zaharko, A. Poole, B. Roessli, and M. Kenzelmann, *Phys. Rev. Lett.* **108**, 077204 (2012).
- [53] G. C. Lau, B. G. Ueland, R. S. Freitas, M. L. Dahlberg, P. Schiffer, and R. J. Cava, *Phys. Rev. B* **73**, 012413 (2006).
- [54] V. O. Garlea, L. D. Sanjeeva, M. A. McGuire, P. Kumar, D. Sulejmanovic, J. He, and S.-J. Hwu, *Phys. Rev. B* **89**, 014426 (2014).
- [55] V. P. Gnezdilov, Y. G. Pashkevich, V. S. Kurnosov, O. V. Zhuravlev, D. Wulferding, P. Lemmens, D. Menzel, E. S. Kozlyakova, A. Y. Akhrorov, E. S. Kuznetsova, P. S. Berdonosov, V. A. Dolgikh, O. S. Volkova, and A. N. Vasiliev, *Phys. Rev. B* **99**, 064413 (2019).
- [56] L. Heinze, H. Jeschke, A. Metavitsiadis, M. Reehuis, R. Feyerherm, J. U. Hoffmann, A. U. B. Wolter, X. Ding, V. Zapf, C. C. Moya, F. Weickert, M. Jaime, K. C. Rule, D. Menzel, R. Valent, W. Brenig, and S. Slow, “Atacamite  $\text{Cu}_2\text{Cl}(\text{OH})_3$ : A model compound for the  $s = 1/2$  sawtooth chain?” (2019), arXiv:1904.07820 [cond-mat.str-el].
- [57] S. R. White and I. Affleck, *Phys. Rev. B* **54**, 9862 (1996).
- [58] S. Eggert, *Phys. Rev. B* **54**, R9612 (1996).
- [59] M. Kumar, Z. G. Soos, D. Sen, and S. Ramasesha, *Phys. Rev. B* **81**, 104406 (2010).
- [60] C. K. Majumdar and D. K. Ghosh, *Journal of Mathematical Physics* **10**, 1388 (1969), <https://doi.org/10.1063/1.1664978>.
- [61] C. K. Majumdar and D. K. Ghosh, *Journal of Mathematical Physics* **10**, 1399 (1969), <https://doi.org/10.1063/1.1664979>.
- [62] W. Caspers and W. Magnus, *Physics Letters A* **88**, 103 (1982).
- [63] P. Di Francesco, P. Mathieu, and D. Senechal, *Conformal field theory* (Springer, 1997).
- [64] I. Affleck, in *Fields, Strings and Critical Phenomena*, edited by E. Brézin and J. Zinn-Justin (North-Holland, Amsterdam, 1990) pp. 563–640, (proceedings of Les Houches Summer School, 1988).
- [65] O. A. Starykh, A. Furusaki, and L. Balents, *Phys. Rev. B* **72**, 094416 (2005).
- [66] D. Sénéchal, in *Theoretical Methods for Strongly Correlated Electrons*, CRM Series in Mathematical Physics, edited by D. Sénéchal, A. M. S. Tremblay, and C. Bourbonnais (Springer, 2004) Chap. 4, pp. 139–186.
- [67] M. A. Tsvetlik, *Quantum field theory in condensed matter physics* (Cambridge university press, 2003).
- [68] A. Metavitsiadis and S. Eggert, *Phys. Rev. B* **95**, 144415 (2017).
- [69] S. Sarkar and D. Sen, *Phys. Rev. B* **65**, 172408 (2002).
- [70] S. Chen, H. Büttner, and J. Voit, *Phys. Rev. B* **67**, 054412 (2003).
- [71] L. Capriotti, F. Becca, S. Sorella, and A. Parola, *Phys. Rev. Lett.* **89**, 149701 (2002).
- [72] S. Chen, H. Büttner, and J. Voit, *Phys. Rev. Lett.* **89**, 149702 (2002).
- [73] T. Giamarchi, *Quantum physics in one dimension* (Oxford science publications, 2004).
- [74] S. Sarkar, *Europhysics Letters (EPL)* **71**, 980 (2005).
- [75] K. Totsuka, *Phys. Rev. B* **57**, 3454 (1998).
- [76] E. Orignac and T. Giamarchi, *Phys. Rev. B* **57**, 5812 (1998).
- [77] O. Derzhko, J. Richter, and M. Maksymenko, *International Journal of Modern Physics B* **29**, 1530007 (2015), <https://doi.org/10.1142/S0217979215300078>.
- [78] C. Wu, D. Bergman, L. Balents, and S. Das Sarma, *Phys. Rev. Lett.* **99**, 070401 (2007).
- [79] D. L. Bergman, C. Wu, and L. Balents, *Phys. Rev. B* **78**, 125104 (2008).
- [80] J. Schnack, H.-J. Schmidt, J. Richter, and J. Schulenburg, *The European Physical Journal B - Condensed Matter and Complex Systems* **24**, 475 (2001).
- [81] H.-J. Schmidt, J. Richter, and R. Moessner, *Journal of Physics A: Mathematical and General* **39**, 10673 (2006).
- [82] G. Vidal, *Phys. Rev. Lett.* **98**, 070201 (2007).
- [83] R. Orús and G. Vidal, *Phys. Rev. B* **78**, 155117 (2008).
- [84] R. B. Griffiths, *Phys. Rev.* **133**, A768 (1964).